Iranian Journal of Materials Science and Engineering, Vol. 20, Number 1, March 2023
RESEARCH PAPER

The Effect of Thermomechanical Treatment on the Microstructure and Mechanical Behavior of an Austenitic Steel Containing 1.4% Al and 17.5% Mn

Mohammad Abankar[1], Hossein Arabi[1,*], Mohammad Taghi Salehi[1], Majid Abbasi[2]

* *arabi@iust.ac.ir*

[1] School of Metallurgy and Materials Engineering, Iran University of Science and Technology, Tehran, Iran
[2] Faculty of Materials and Industrial Engineering, Babol Noshirvani University of Technology, Mazandaran, Iran

Received: August 2022 **Revised: February 2023** **Accepted: March 2023**
DOI: 10.22068/ijmse.2937

Abstract: *The aim of this research was to evaluate the effect of different thermomechanical treatments on the microstructure and investigate some of the mechanical properties of a TWIP steel rich in Mn & Al. To this end, a block of a TWIP steel with nominal composition Fe-17.5Mn-1.36Al-0.8C was cast and then subjected to hot rolling followed by cold rolling and heat treatment. Cold rolling was performed before heat treatment in order to reduce grain size and improve the tensile and fatigue properties. X-ray diffraction technique was used before and after the heat treatment to study the structure of the phases present in the microstructure. No sign of martensitic transformation after cold deformation was observed. However, by increasing the amount of cold deformation, the number of mechanical twins and slip bands increased, which resulted to an increase in hardness and strength values. The best tensile and fatigue result was obtained after 47% thickness reduction and annealing at 715˚C for 10 min. Under these conditions, the mean grain size reduced from 138 to 9 µm resulting in an increase in yield strength from 395 to 510 MPa; and the fatigue life improvement from the mean life of 10200 for the cast sample to 21500 cycles for the treated sample, when these samples underwent fatigue tests at a stress range of 650 MPa and R=0 (i.e., $\sigma_{min} = 0$). In addition, the diameter and depth of dimples in fracture surfaces decreased by reducing the grain size, so the fracture mode remained ductile, and an adequate plastic deformation occurred before failure.*

Keywords: *TWIP steel, Heat Treatment, Fatigue, Fractography, Thermomechanical processing.*

1. INTRODUCTION

Metals can be plastically deformed by either slip (dislocation gliding), twining, or both mechanisms. The microstructure of metal significantly affects its mechanical properties [1]. Plasticity induced by the transformation of austenite to martensite during mechanical work is known as (TRIP). Worth mentioning that the TRIP phenomenon may occur by a twinning mechanism known as twinning-induced plasticity (TWIP) [1, 2].

Generally, twinning with the volumetric strains has a lower effect on the work hardening capacity than planar plasticity of slipping, which produces the highest dislocation density [3]. Nowadays, it is known that twinning is the main plastic deformation mechanism in austenitic manganese steels. Thus, one should bear in mind that different parameters' contributions to plasticity and tensile behavior are crucial for developing and processing new alloys. Over the past two decades, alloys designed on the base of Fe-Mn-C [4], Fe-Mn-Al-C [5], and Fe-Mn-Al-Si-C [6] systems which have different alloying contents and developed by various processing techniques. Most of these alloys have twinning-induced plasticity (TWIP) behavior. The outstanding properties of TWIP steels come from their high strain hardening rate due to the numerous mechanical twins generated during plastic deformation [1-3]. Therefore, twin boundaries similar to grain boundaries can act as strong barriers against dislocation motion [4, 5], and also contribute to decreasing the effective grain size [6-9]. In recent decades, Fe- Mn-Al-Si-C-alloys, especially those with a high amount of manganese (15-30%), have attracted significant attention due to their remarkable mechanical properties, such as high strength and excellent ductility. Among these alloys, twinning-induced plasticity steels (TWIP) have extraordinary strength and ductility, resulting from thermomechanical processing such as hot rolling and different consequent cycles of both heating and cooling [10-14]. These face-centered cubic austenitic steels have gained a particular interest in the automobile industry and it is used widely as structural components [15]. The process of alloying and thermomechanical treatment resulted in low stacking fault energy

[DOI: 10.22068/ijmse.2937]

from 20 to 50 mJ m^{-2} at room temperature [16] and high strain hardening rates which ended in the production of proper TWIP steel for engineering needs [17, 18]. Grassel et al [19] evaluated some of the mechanical properties of Fe–25Mn–3Si–3Al and Fe–30Mn–3Si–3Al steels. They found that their uniform elongations are about 80% and their UTS is approximately 600 MPa, which is suitable for automotive industries. El-Danaf and colleagues [20-22] investigated the strengthening effect of grain size on the mechanical properties of Fe–31%Mn–3%Al–3%Si TWIP steel. These researchers stated that this type of steel with a small grain size is very suitable for automotive applications. On the other hand, some other researchers studied some of the TWIP steels with various amounts of carbon in their composition. They figured out that the uniform elongation of about 60% and UTS of more than 1.1 GPa can be obtained in these steels. They reported that grain refinement significantly prevents mechanical twinning. Moreover, other researchers [23-25] claimed that fine grains might suppress the formation of twinning and martensite in low SFE materials. Austenitic steels with a high amount of Mn usually have a notable strain hardening rate because of the increase in dislocation density during deformation. However, strengthening is generally accompanied by a reduction in plasticity, i.e., a drop in elongation occurs. Different researchers carried out various suitable heat treatments to investigate the relation between microstructure, strength, and plasticity [9, 26-28]. For example, Kang et al. [29] evaluated the influence of temperature on the mechanical properties and microstructure of a cold-worked Fe-18Mn-0.6C-1.5Al. They stated that after 60% cold reduction, the recrystallization process can be initiated at 600˚C and finished at 700˚C at 10 minutes. Additionally, Curtze and colleagues [30] studied the microstructure of various TWIP steel plates reported that SFE could affect the hardening behavior of the steel. They stated that alloys with lower SFE exhibit high strength and ductility.

This work aims to reveal not only the tensile behavior of a TWIP steel that has undergone various thermo-mechanical processes but also the effect of grain size on the fatigue behavior of this steel. This austenitic steel contains a high amount of Mn and 1.3% wt Al.

2. EXPERIMENTAL PROCEDURE

An alloy with the chemical composition shown in Table 1 was cast in an induction melting furnace under an Ar atmosphere in the shape of a Y-block, having 100 Kg weight. The thickness of the Y-block was 3 cm. Stacking fault energy (SFE) of Y- block was measured using the major elements of the composition, i.e., Ni and Mn, according to the equation reported by Allain et al [16, 31] that indicated as Eq. 1.

$$\gamma = 2\rho\Delta G^{\gamma\to\varepsilon} + 2\sigma_{\gamma\to\varepsilon} \quad (1)$$

When $\Delta G^{\gamma\to\varepsilon}$ is the free molar enthalpy of the transformation $\gamma \to \varepsilon$, ρ the molar surface density of atoms in the {1 1 1} planes and $\sigma_{\gamma\to\varepsilon}$ the energy per surface unit of a {1 1 1} interface between γ and ε.

The cast block was initially homogenized at 1200˚C, and then its thickness was reduced to 5.7 mm by the hot rolling in 5 passes (77% reduction of cross-section area) at 1200˚C. The hot-rolled samples were annealed at 1100˚C for 30 min. Several samples from the hot rolled and annealed materials were cut off and subjected to asymmetric cold rolling in order to reduce the thickness from 5.7 to 4.8, 4.3, 3.7, and 3 mm. i.e., 15, 25, 35, and 47% reduction in thickness. Finally, the samples were heat-treated at 715˚C for different times of 10, 20, and 30 min.

Table 1. Mean chemical composition of TWIP steel, used in this research.

Sample	Chemical composition (wt.%)				
TWIP steel	Fe	Mn	Al	Si	C
	79.50	17.50	1.36	0.85	0.79

All the samples were coded on the based on the percentage of cold-rolled reduction and annealing time, as shown in Table 2. Microstructural analysis of each sample was carried out using an optical microscope (MEJI- MA326) and scanning electron microscope (Roventec vega II XMU-Tescan). X-ray diffraction technique (BOURE VESTNIK- DRON-8) with CuKα= 1.5428 Å was utilized to evaluate phase formation. The mean grain size of various samples was measured using OM images, standard ASTM E112, and MIP image analyzer software. The tensile tests were performed according to the standard ASTM E8M. A few fatigue tests were carried out at a stress range of 650 MPa under the condition of R=0 (i.e., $^{\sigma_{min}}/_{\sigma_{max}} = 0$) via the INSTRON 8502 machine. Fractography analysis for both tensile

[DOI: 10.22068/ijmse.2937]

and fatigue samples was carried out via SEM. Vickers microhardness method was used according to standard ASTM E384 in order to establish the effect of cold rolling and annealing processes on microstructures.

3. RESULTS AND DISCUSSIONS

3.1. Cold Rolling Microstructure

The result of the XRD analyzer for the sample subjected to asymmetric cold rolling after 16, 24, 35, and 47% reduction in thickness are presented in Fig.1. As one can see in this figure increase in the amounts of cold deformation did not cause the transformation of austenite to martensite and the microstructure is fully austenitic.

Optical images from the microstructures presented in figure 2 show a significant amount of slip bands in some high atomic density planes of the grains. These high amount of slip bands is an indication of formation of a huge mobile dislocation on high-density planes of the grains after rolling. Due to the low Stacking Fault Energy (SFE) of this type of steel [7], one expects some plastic deformation to occur with mechanical twinning during cold rolling. Although in Figs (2 & 3) twinning can hardly be observed, by increasing the amounts of deformation, it seems an increase in the dislocation population occurred, to the limit of its saturation, so that the deformation continued by increasing the twinning population, leading to the higher amount of SFE in the samples. The researcher thinks the type of etchant used for these samples was not adequate for revealing the twins properly, and it is recommended that one examines different etchants for revealing the twins in this type of steels.

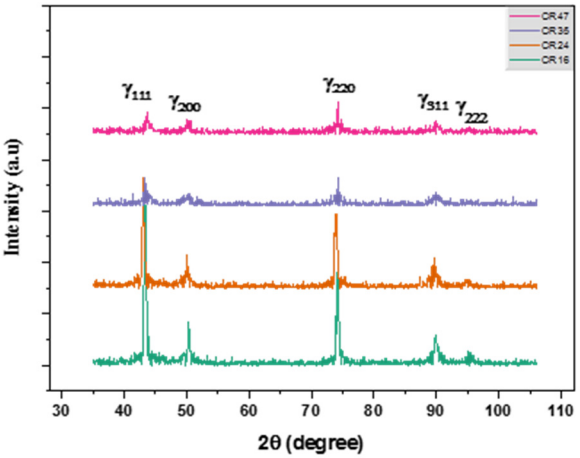

Fig. 1. XRD pattern of the samples after cold rolling to different thickness reductions.

Table 2. The details of heat treatments and samples codes.

Test No.	Sample Code	Rolling Conditions %of reduction	Heat Treatment Conditions	
			Annealing Temperature (˚C)	Annealing Time (Min)
1	CA	-	1100	60
2	HR	77% Hot Rolled	1200	30
3	HRA	77% Hot Rolled	1100	10
4	CR16	16% Cold Rolled		
5	CR24	24% Cold Rolled		
6	CR35	35% Cold Rolled		
7	CR47	47% Cold Rolled		
8	CR16A10	15% Cold Roll	715	10
9	CR16A20			20
10	CR16A30			30
11	CR24A10	25% Cold Roll		10
12	CR24A20			20
13	CR24A30			30
14	CR35A10	35% Cold Roll		10
15	CR35A20			20
16	CR35A30			30
17	CR47A10	47% Cold Roll		10
18	CR47A20			20
19	CR47A30			30

HR=hot rolled
CR=cold rolled
CA=cast and annealed

CRA=cold rolled + annealed
HRA=hot rolled + annealed

[DOI: 10.22068/ijmse.2937]

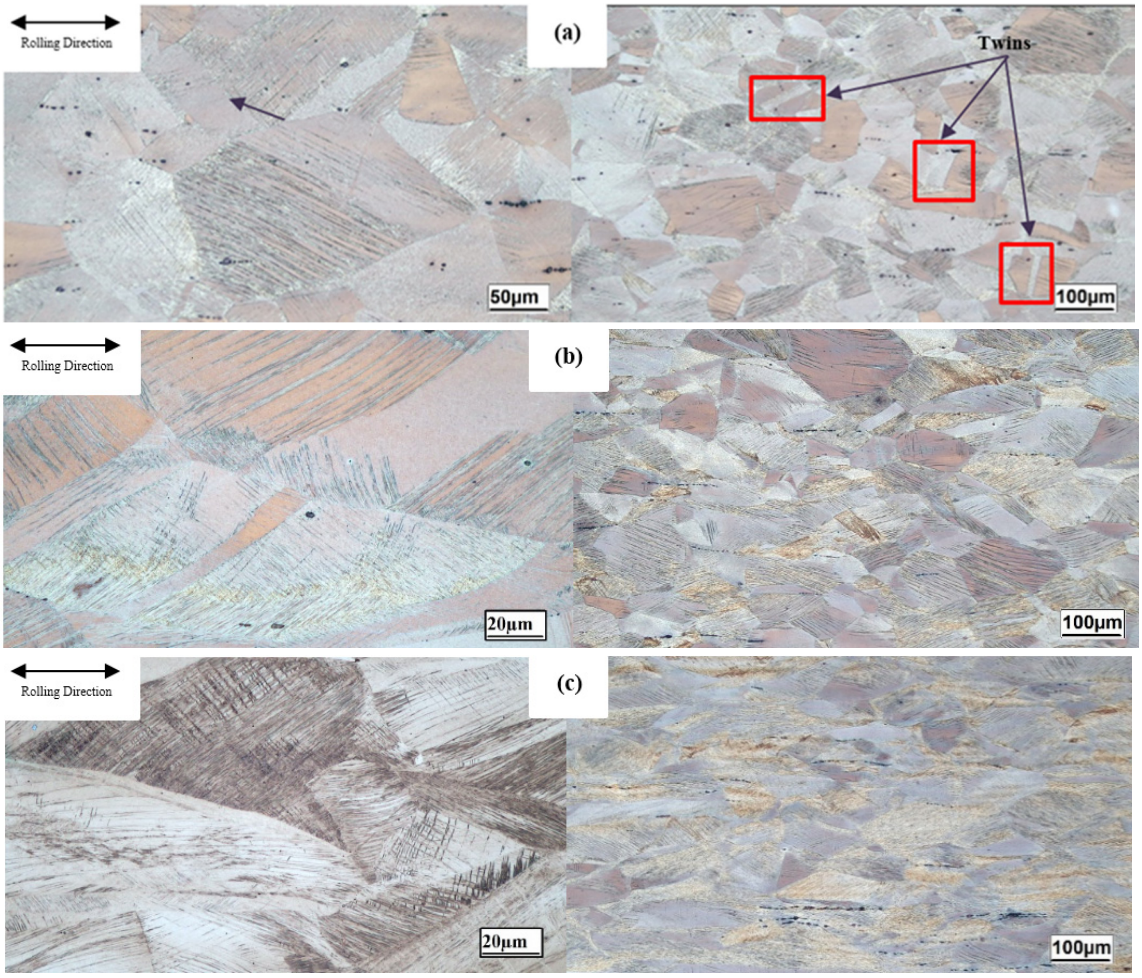

Fig. 2. Optical microscopy images from microstructure of (a) CR16, (b) CR24, (c) CR35, and (d) CR47.

Some researchers said [32] that twins can be formed with a higher density of slip bands in grains with a high density of dislocations. An example of the formation of such twins can be seen in Fig 3 (b). The formation of twins in the planes having high amounts of mobile dislocations (i.e. {111}) needs further study by TEM, and this phenomenon was not studied in this research due to lack of access to TEM. Various micrographs in Fig. 3 show by increasing the amount of deformation, a more significant amount of cross slip and twinning occurred, which means the amount of dislocations interaction increased, and further twinning also occurred, leading to further improvement in the strength of the alloy.

3.2. Annealing Microstructure

As mentioned before, all the cold rolled samples were annealed at 715˚C for 10, 20, and 30 minutes. Figure 4 shows variation in the mean size of the grains after annealing the cold rolled samples. Increasing the strain reduced the average size of the grains after annealing. By increasing the annealing time from 10 to 30 min, the microstructures of the samples CR24A, CR35A, and CR47A became coarser. Grain Coarsening might have occurred due to secondary recrystallization, as this phenomenon reported in Ref. [29], thus leading to the formation of abnormal grains growth [10]. The finer the grains within the microstructure, the higher the number of grain boundaries which, according to the rule of Hall and Petch [8], the sample grains' higher strength. Also, one should bear in mind that the increase in strength is not only due to an increase in dislocation density and formation of smaller grains during annealing but also due to the formation of twins. For example, the twin boundaries, depicted in micrographs shown in Fig.5, related to the cold rolled 16% and the annealed to 10, 20, and 30 min at 715˚C.

[DOI: 10.22068/ijmse.2937]

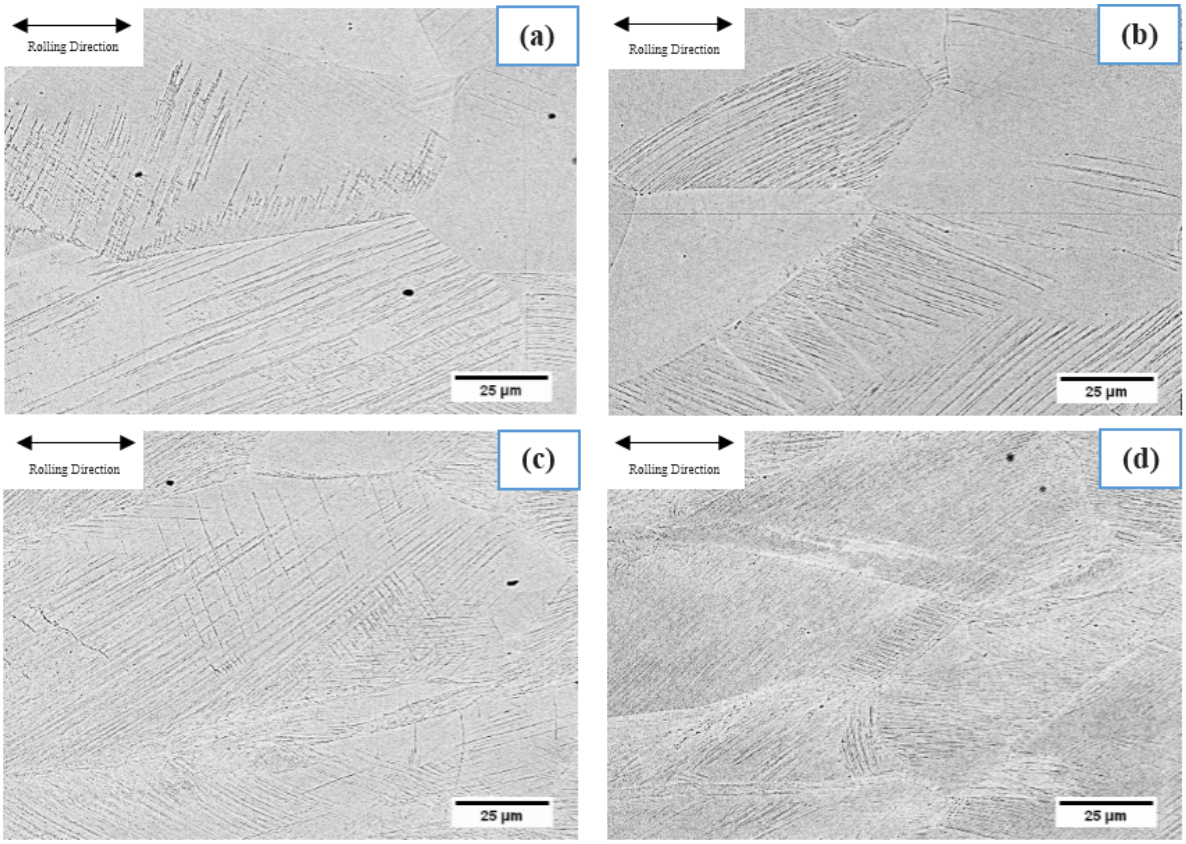

Fig. 3. SEM images from microstructure of (a) CR16, (b) CR24, (c) CR35, and (d) CR47.

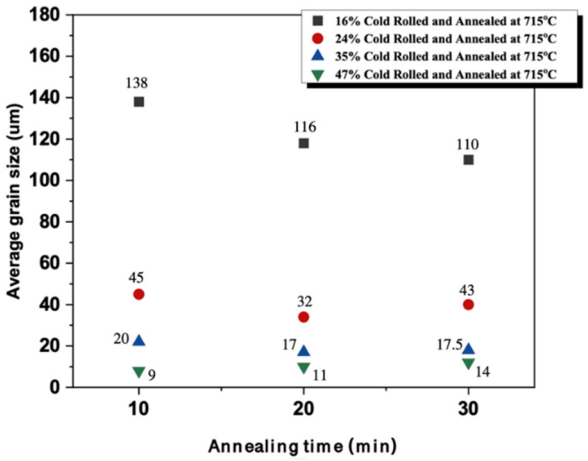

Fig. 4. The average grain size of different samples.

Recrystallized grains in these samples, i.e., CR16A20 and CR16A30, are stated in high angle and twin boundaries. However, the volume fraction of recrystallized grain is low, perhaps due to an incomplete recrystallization process because of the shortage of time. As illustrated in Fig. 5, variation in the number of slip bands and their directions within high-density plans (i.e. {111}) of one of the grains can indicate that more than one slip system has been activated higher amount of deformation. The more intersections of the slip bands seem to form more suitable locations for the nucleation of recrystallized grains. Thus, it seems some of the recrystallized grains occurred within the deformed grains instead of the grain boundaries, where the slip bands interacted, as shown in Fig. 6.

The micrograph presented in Fig. 6 shows some recrystallized grains that occurred within the grains at the interface of twins, which had no slip bands, for example, location (A) in Fig. 6(a). This observation is in good agreement with the results that previous research published [67] Recrystallization in the samples annealed after a 35% reduction seems to be almost completed. Although some signs of heterogeneity in recrystallized regions existed, as shown in Fig. 7. The heterogeneity may be due to the formation of various textures developed during cold work. This need, of course, further investigation to relate somehow this heterogeneity observed with the various probable texture developed. Various images in Fig. 8 show the microstructure of the samples CR47A10, CR47A20, and CR47A30 indicating fully recrystallized grains.

[DOI: 10.22068/ijmse.2937]

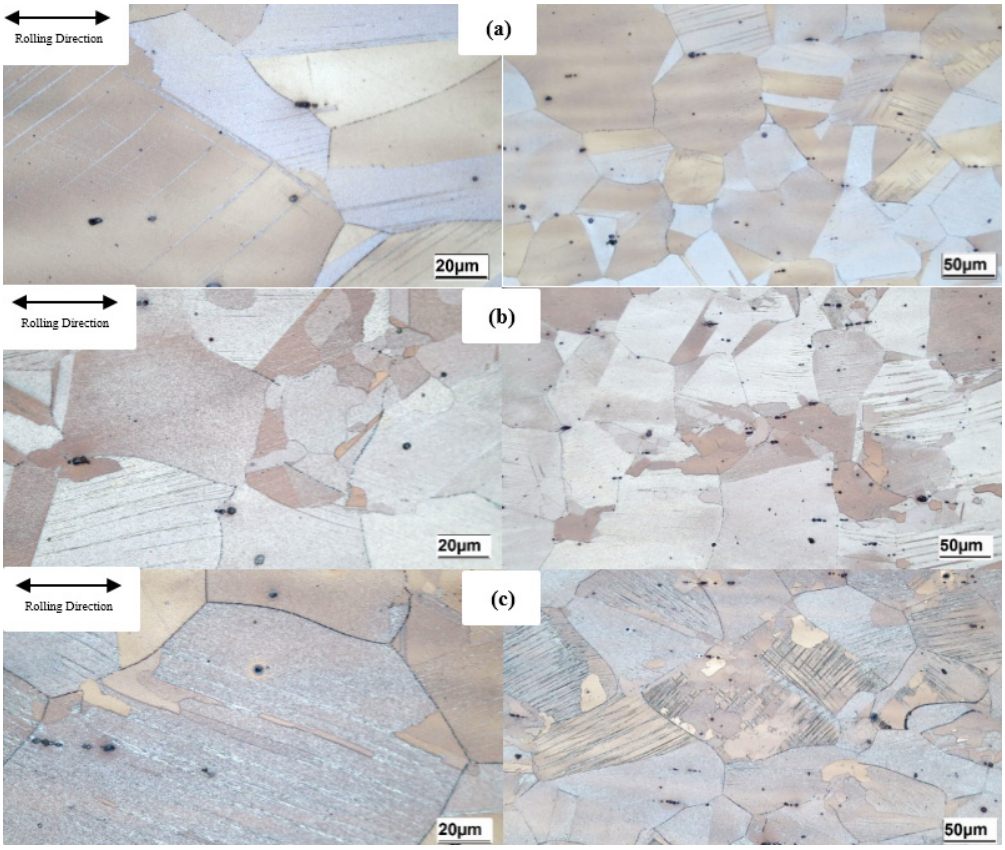

Fig. 5. Optical microscope images from microstructure of (a) CR16A10, (b) CR16A20, and (c) CR16A30.

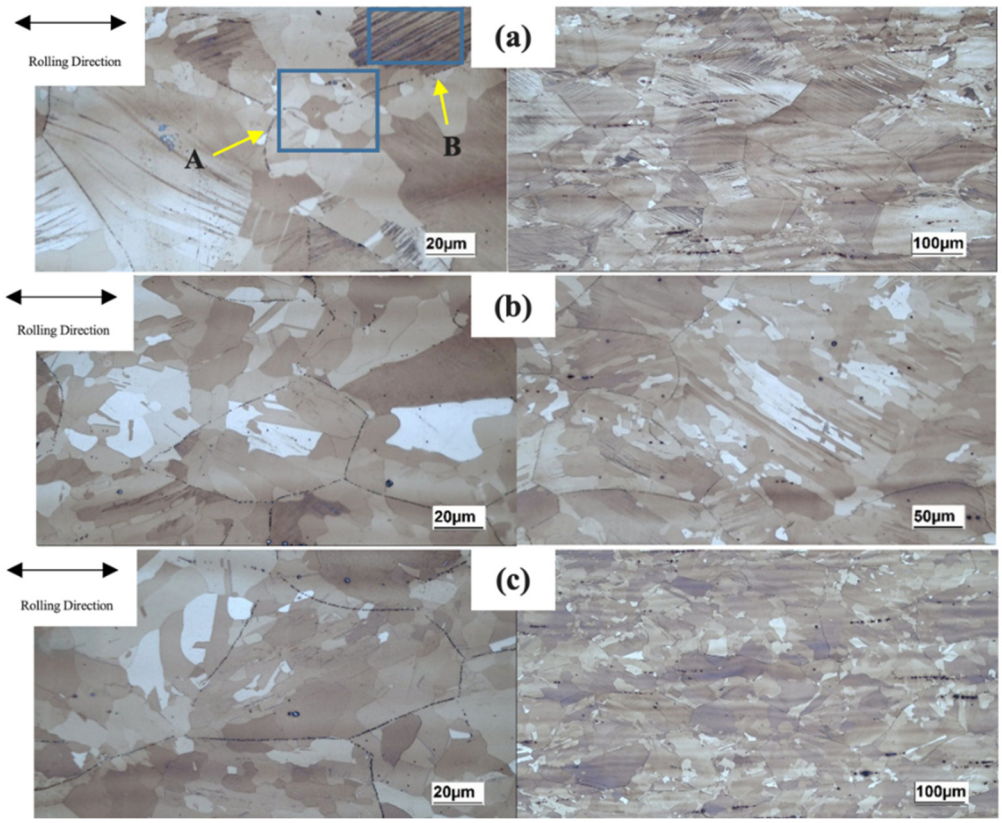

Fig. 6. Optical microscope images from microstructure of (a) CR24A10, (b) CR24A20, and (c) CR24A30.

[DOI: 10.22068/ijmse.2937]

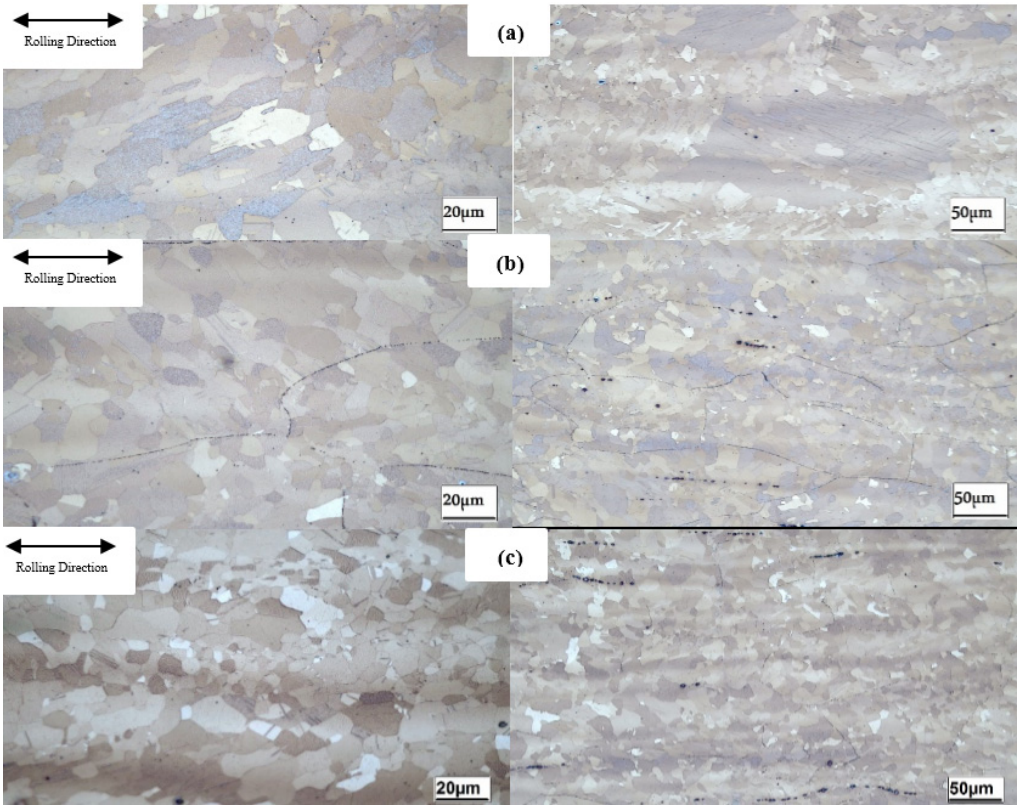

Fig. 7. Optical microscope images from microstructure of (a) CR35A10, (b) CR35A20, and (c) CR35A30.

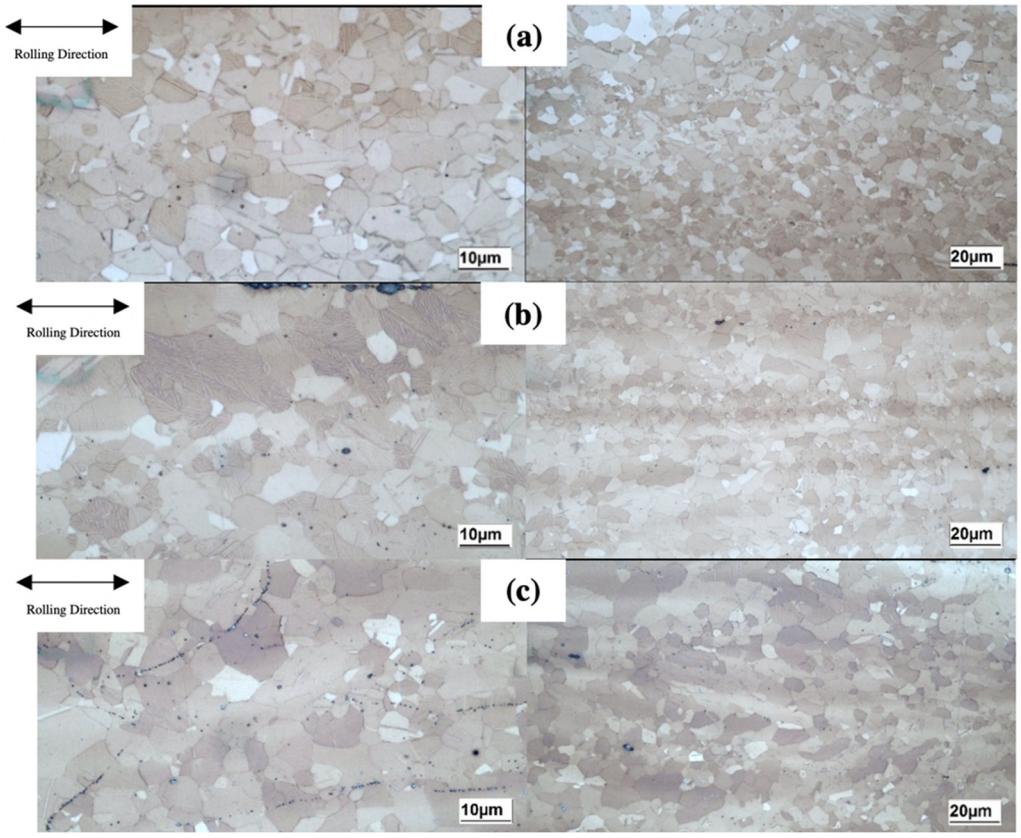

Fig. 8. Optical microscope images from microstructure of samples (a) CR47A10, (b) CR47A20, and (c) CR47A30.

[DOI: 10.22068/ijmse.2937]

It has been stated [33] that recrystallized regions of microstructure can play a key role in some mechanical properties of alloys analysis of the above-mentioned samples shown in Fig. 9 indicates that the heat-treated samples' microstructure is fully austenitic.

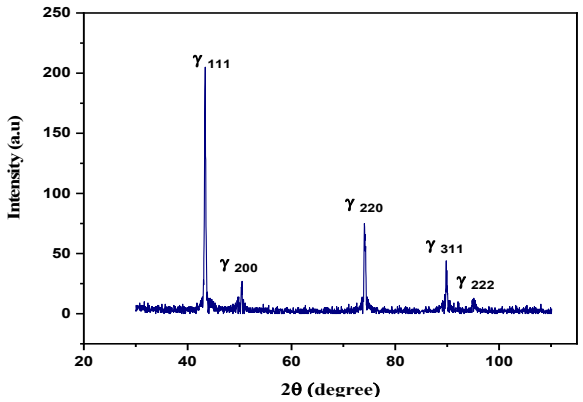

Fig. 9. Typical XRD pattern of sample CR47A10.

3.3. Mechanical Properties

3.3.1. Hardness

The results of microhardness tests for various samples are shown in Fig. 10. The hardness of the rolled samples has improved due to likely increased dislocation densities and mechanical twinning formation [28]. Still, after annealing the samples, for example, CR48A10, the hardness diminished substantially due to probably reduced dislocation densities and new grains or sub-grains formed. Nucleation of these new grains occurred at twin boundaries and grain boundaries as they contained higher energy than the rest of the matrix, according to Ref. [34].

3.3.2. Tensile test

The result of some of the tensile tests performed under a strain rate of 0.001 s^{-1} has been illustrated in Fig. 11 and Table 3. These results show sample CR16A10 had higher yield strength and lower elongation than the other recrystallized samples, probably because of more microstructure stability at this temperature. Worth mentioning various researchers investigated the relationship between the high work hardening rate of TWIP alloys and mechanical twins and reported that mechanical twins contain a high amount of sessile (i.e., immobile) dislocations, acting as strong barriers for movements of glide dislocation at high strain rates [6, 7]. But these dislocations can climb at high temperatures resulting in softening of alloy. Hence an improvement in ductility and reduction in yield will occur. Thus, according to this analysis, the result of tensile tests carried out in this research (Fig. 11) can be justified.

The partially recrystallized microstructure can be observed in samples CR24A10 and CR35A10. It seems the amounts of deformed regions and mechanical twinning density in these samples declined and was replaced by recrystallized grains. Since the density of recrystallized grains increased, the ductility of the alloy increased too, and therefore one can say that by raising the volume fraction of recrystallized grains, the strength of the alloy must decline; the result shown in Table 3 confirms this. Annealing at 715˚C for 10 minutes after a thickness reduction of up to 47% caused the yield strength to improve slightly.

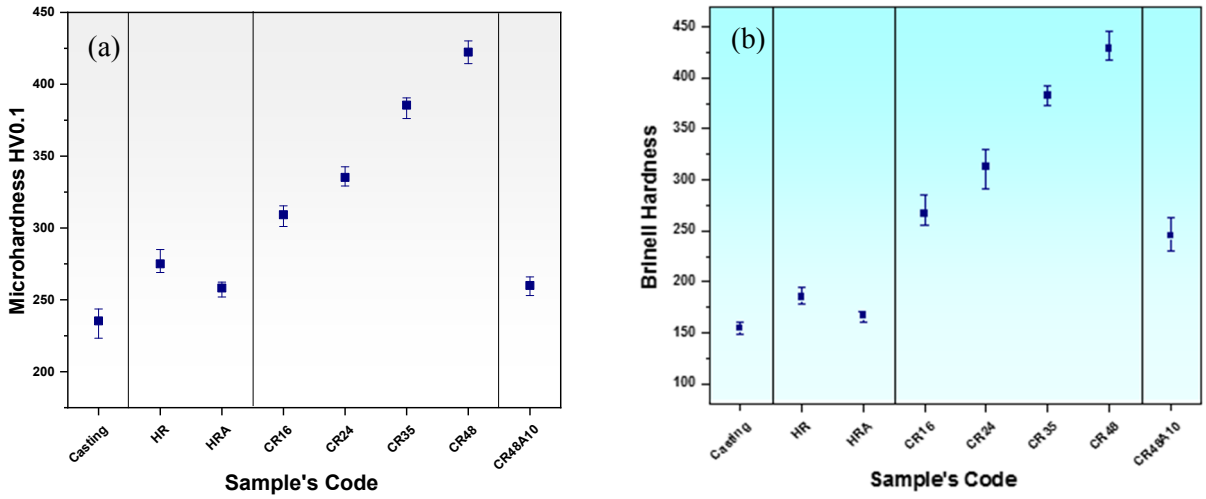

Fig. 10. (a) The results of vicker microhardness tests for different samples, (b) Brinell hardness for different samples.

[DOI: 10.22068/ijmse.2937]

Table 3. UTS, US, and elongation of different samples.

sample	UTS (MPa)	YS (MPa)	Elongation (%)
HRA	777.52	395.2	97
CR16A10	870.37	603.25	70
CR24A10	859.33	476.74	78
CR35A10	850.11	476.56	83
CR47A10	819.69	509.55	87

This improvement might be due to finer grains produced during cold work and annealing. These grains have obviously higher stored energy and can increase yield strength. One should bear in mind that more grain boundaries existing in finer grains structures can act as obstacles for dislocation movement, leading to enhancement in yield strength [29, 33, 35].

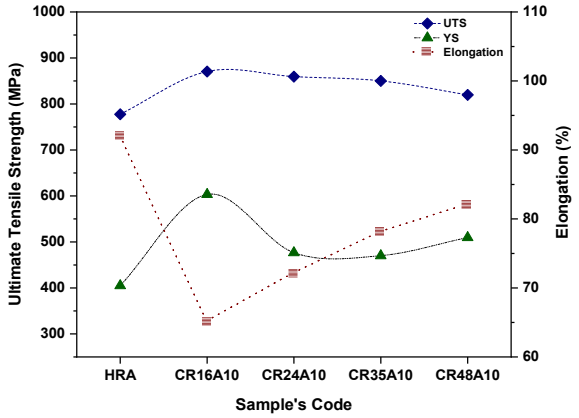

Fig. 11. Various flow properties, UTS, YS, and elongation of different samples.

3.4. Fractography

SEM images of the fracture surfaces of different samples are shown in Fig. 12. The amount of elongation of the samples shown in Table 3 and the presence of dimples in the fracture surface of all samples indicates that the fracture mode of all samples is ductile. The different sizes of dimples have been said to have a direct relationship with the grain size of the sample [20, 36]. For example, the mean size of dimples in the HRA sample with a mean grain size of 138 μm is larger than those in the CR47A10 sample with a mean grain size of 8 μm. Some researchers [37, 38] have stated that unsolved precipitates and nonmetallic inclusions between fine and coarse dimples can be suitable places for the nucleation of coarse dimples. It should be noted that in some parts of the fracture surface, for example, in the samples CR16A10, CR24A10, CR35A10, and CR47A10 shear mode of fracture occurred. Forming of shear mode can be due to a localized increase of strength at some parts of the samples due to dislocation accumulation, resulting in shear mode at fracture. The fractured samples showed, in spite of a large amount of elongation at failure, these elongations occurred homogeneously as no localized plastic deformation was observed along gauge lengths of the samples. So that one can hardly see the necking phenomenon along the gauge length of the samples, as shown in Fig. 13. It has also been reported [39] that the deformation twins are obstacles for dislocation movements, therefore it seems due to the formation of these twins during the deformation of the samples when they were subjected to tensile test, and the slight amount of necking observed along the gage length, one can assume that necking could not progress by the application of more strain because these twins boundaries which restricted the movement of dislocations; so that sever work-hardening occurred.

3.5. Fatigue

Fig. 14 shows the typical fatigue fracture surface of the samples, within which striations and secondary cracks can be observed. Secondary cracks are an indication of crack branching during second stage of crack growth. These cracks can accelerate the cracking procedure. The crack propagation direction varied during fracture propagation and maybe it is due to the occurrence of dynamic strain aging phenomenon due to stress concentration in some regions of the specimen which resulted in both formation of secondary cracks and a change in propagation direction at the second stage of crack propagation. In other words, stress concentration in some regions can act as an arresting point and reduces the movement of the crack tip, hence the formation of secondary cracks and change in crack direction. In addition, concentration around the crack tip can lead to the formation of mechanical twins, increasing work hardening.

According to some references [41-43], this can

[DOI: 10.22068/ijmse.2937]

provide the required stress for changing the propagation direction of fatigue crack. However, if the deformation twins do not form during fatigue, the reason for the cessation of crack propagation can be due to the dynamic strain aging mechanism [43].

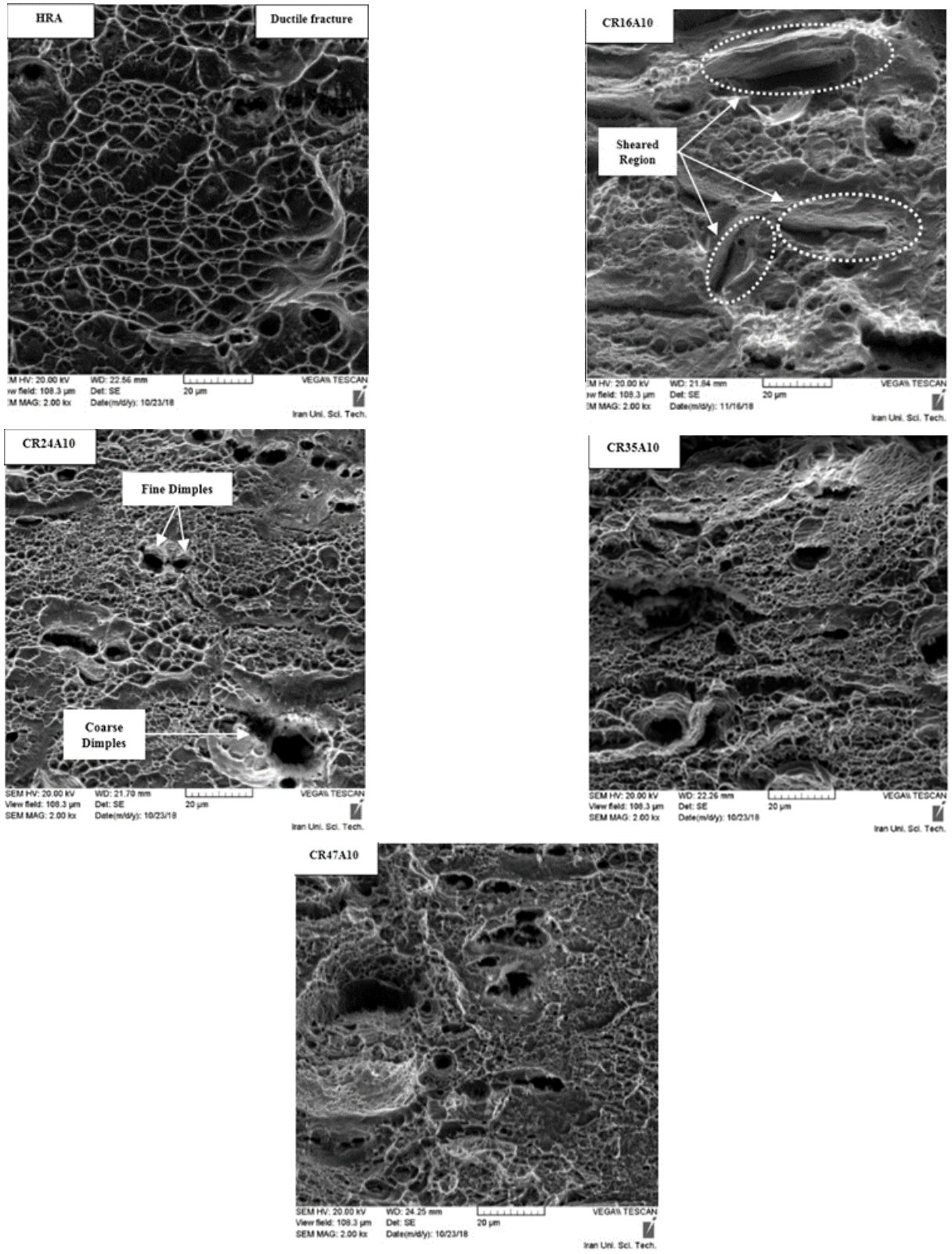

Fig. 12. The fracture surfaces of different sample

[DOI: 10.22068/ijmse.2937]

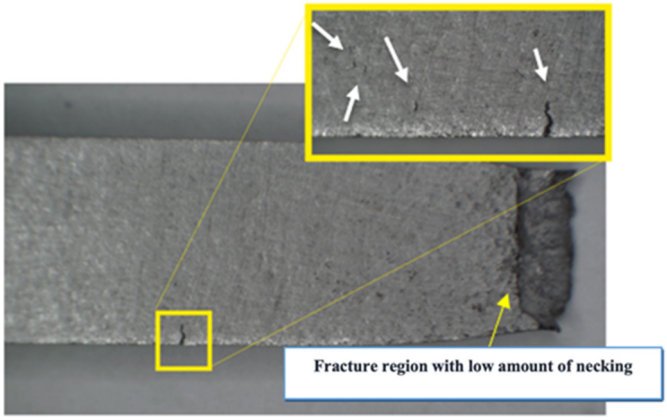

Fig. 13. Typical gauge length of the samples subjected to tensile test, after fracture.

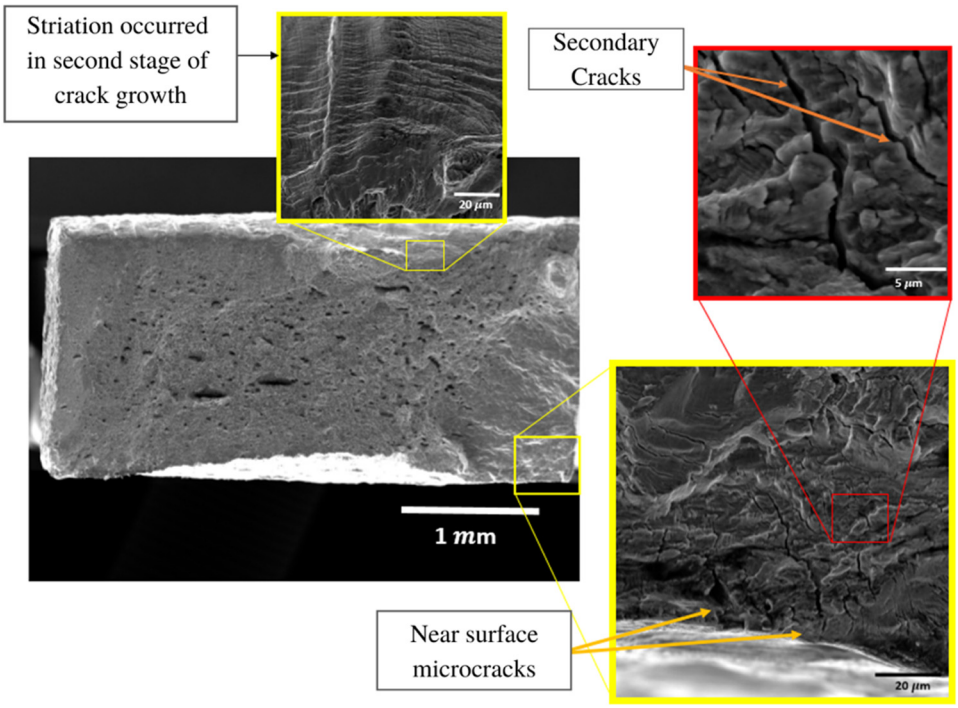

Fig. 14. Typical fatigue fracture surface of the HRA sample.

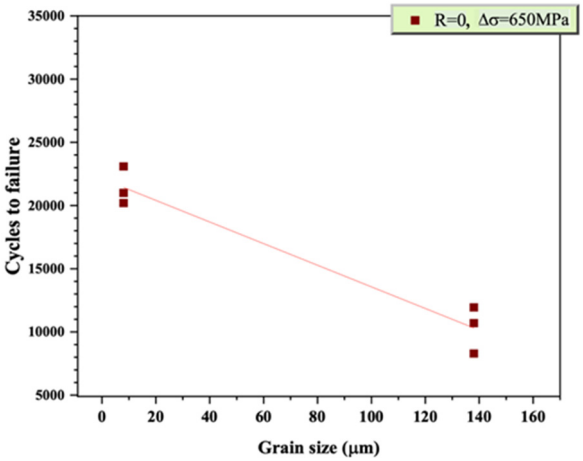

Fig. 15. increasement of fatigue life due to reduction of grain size

4. CONCLUSIONS

1- Asymmetrical cold rolling caused a significant increase in the hardness values. The Vicker hardness of the assymetrical cold rolled sample (CR47) reached 425 HV compared to Hot rolled annealed sample (265 HV).

2- Thermomechanical treatment of the alloy caused an improvement in the flow properties of the alloy, i.e., UTS, YS, and elongation; the yield strength of the CR47A10 sample was about 22% more than HRA. The ultimate strength of CR47A10 and HRA were about 777 and approximately 820 MPa, and the elongation of CR47A10 was improved by

[DOI: 10.22068/ijmse.2937]

87% compared with the HRA sample.

3- By decreasing the grain size, the fatigue life improved substantially, e.g., it increased from 10200 cycles to 25000 cycles in the sample CR47A10, which was cold-rolled for 47% and annealed for 10 min at 715˚C.

REFERENCES

[1]. Jin, J.-E. and Y.-K. Lee, Strain hardening behavior of a Fe–18Mn–0.6 C–1.5 Al TWIP steel. Materials Science and Engineering: A, 2009. 527(1-2): p. 157-161.

[2]. D.T. Pierce, J.A. Jiménez, J. Bentley, D. Raabe, C. Oskay, J.E. Wittig, The influence of manganese content on the stacking fault and austenite/ε-martensite interfacial energies in Fe–Mn–(Al–Si) steels investigated by experiment and theory. Acta Materialia, 2014. 68: p. 238-253.

[3]. Song, W., T. Ingendahl, and W. Bleck, Control of strain hardening behavior in high-Mn austenitic steels. Acta Metallurgica Sinica (English Letters), 2014. 27(3): p. 546-556.

[4]. Gutiérrez-Urrutia, I. and D. Raabe, Multistage strain hardening through dislocation substructure and twinning in a high strength and ductile weight-reduced Fe–Mn–Al–C steel. Acta Materialia, 2012. 60(16): p. 5791-5802.

[5]. Gutierrez-Urrutia, I. and D. Raabe, Dislocation and twin substructure evolution during strain hardening of an Fe–22 wt.% Mn–0.6 wt.% C TWIP steel observed by electron channeling contrast imaging. Acta Materialia, 2011. 59(16): p. 6449-6462.

[6]. Sevillano, J.G., An alternative model for the strain hardening of FCC alloys that twin, validated for twinning-induced plasticity steel. Scripta Materialia, 2009. 60(5): p. 336-339.

[7]. H. Idrissi, K. Renard, L. Ryelandt, D. Schryvers, P.J. Jacques, On the mechanism of twin formation in Fe–Mn–C TWIP steels. Acta Materialia, 2010. 58(7): p. 2464-2476.

[8]. Pande, C., B. Rath, and M. Imam, Effect of annealing twins on Hall–Petch relation in polycrystalline materials. Materials Science and Engineering: A, 2004. 367(1-2): p. 171-175.

[9]. Pavel Kusakin, Andrey Belyakov, Christian Haase, Rustam Kaibyshev, Dmitri A. Molodov, Microstructure evolution and strengthening mechanisms of Fe–23Mn–0.3 C–1.5 Al TWIP steel during cold rolling. Materials Science and Engineering: A, 2014. 617: p. 52-60.

[10]. O Grässel, L Krüger, G Frommeyer, L.W Meyer, High strength Fe–Mn–(Al, Si) TRIP/TWIP steels development—properties—application. International Journal of plasticity, 2000. 16(10-11): p. 1391-1409.

[11]. Hui-Zhen Wang, Ping Yang, Wei-Min Mao, Fa-Yun Lu, Effect of hot deformation of austenite on martensitic transformation in high manganese steel. Journal of alloys and compounds, 2013. 558: p. 26-33.

[12]. O. Bouaziz, S. Allain, C.P. Scott, P. Cugy, D. Barbier, High manganese austenitic twinning induced plasticity steels: A review of the microstructure properties relationships. Current opinion in solid state and materials science, 2011. 15(4): p. 141-168.

[13]. M. Eskandari, M. A. Mohtadi-Bonab, A. Zarei-Hanzaki & S. M. Fatemi, Effect of Hot Deformation on Texture and Microstructure in Fe-Mn Austenitic Steel During Compression Loading. Journal of Materials Engineering and Performance, 2018. 27(4): p. 1555-1569.

[14]. Mahmoud Gadelhaq, Atef S. Hamada, M.A Hassan, Jukka Kömi, Dynamic energy absorption of ultrafine-grained TWIP steel under axial impact loading. International Journal of Computational Physics Series, 2018. 1(1): p. 51-64.

[15]. Christian Haase, Luis A. Barrales-Mora, Franz Roters, Dmitri A. Molodov, Günter Gottstein, Applying the texture analysis for optimizing thermomechanical treatment of high manganese twinning-induced plasticity steel. Acta materialia, 2014. 80: p. 327-340.

[16]. S. Allain, J.-P. Chateau, O. Bouaziz, S. Migot, N. Guelton, Correlations between the calculated stacking fault energy and the plasticity mechanisms in Fe–Mn–C alloys.

[DOI: 10.22068/ijmse.2937]

Materials Science and Engineering: A, 2004. 387: p. 158-162.
[17]. De Cooman, B., O. Kwon, and K.-G. Chin, State-of-the-knowledge on TWIP steel. Materials Science and Technology, 2012. 28(5): p. 513-527.
[18]. Bleck, W. and K. Phiu-On. Microalloying of cold-formable multi phase steel grades. in Materials Science Forum. 2005. Trans Tech Publ.
[19]. Grässel, O. and G. Frommeyer, Effect of martensitic phase transformation and deformation twinning on mechanical properties of Fe–Mn–Si–AI steels. Materials science and technology, 1998. 14(12): p. 1213-1217.
[20]. Singon Kang, Jae-Gil Jung, Mihyun Kang, Wanchuck Woo, Young-Kook Lee, The effects of grain size on yielding, strain hardening, and mechanical twinning in Fe–18Mn–0.6 C–1.5 Al twinning-induced plasticity steel. Materials Science and Engineering: A, 2016. 652: p. 212-220.
[21]. Gutierrez-Urrutia, I. and D. Raabe. Study of deformation twinning and planar slip in a TWIP steel by Electron Channeling Contrast Imaging in a SEM. in Materials Science Forum. 2012. Trans Tech Publ.
[22]. Jiménez, J.A. and G. Frommeyer, Analysis of the microstructure evolution during tensile testing at room temperature of high-manganese austenitic steel. Materials Characterization, 2010. 61(2): p. 221-226.
[23]. El-Danaf, E., S.R. Kalidindi, and R.D. Doherty, Influence of grain size and stacking-fault energy on deformation twinning in fcc metals. Metallurgical and Materials Transactions A, 1999. 30(5): p. 1223-1233.
[24]. Asgari, S., Anomalous plastic behavior of fine-grained MP35N alloy during room temperature tensile testing. Journal of materials processing technology, 2004. 155: p. 1905-1911.
[25]. G. Dini, A. Najafizadeh, R. Ueji, S.M. Monir-Vaghefi, Tensile deformation behavior of high manganese austenitic steel: The role of grain size. Materials & Design, 2010. 31(7): p. 3395-3402.
[26]. Alexander Kalinenko, Pavel Kusakin, Andrey Belyakov, Rustam Kaibyshev, Dmitri A. Molodov, Microstructure and mechanical properties of a high-Mn TWIP steel subjected to cold rolling and annealing. Metals, 2017. 7(12): p. 571.
[27]. Torganchuk, V., A. Belyakov, and R. Kaibyshev, Effect of rolling temperature on microstructure and mechanical properties of 18% Mn TWIP/TRIP steels. Materials Science and Engineering: A, 2017. 708: p. 110-117.
[28]. Z. Yanushkevich, A. Belyakov, C. Haase, D.A. Molodov, R. Kaibyshev, Structural/textural changes and strengthening of an advanced high-Mn steel subjected to cold rolling. Materials Science and Engineering: A, 2016. 651: p. 763-773.
[29]. Singon Kang, Yeon-Seung Jung, Joong-Hwan Jun, Young-Kook Lee, Effects of recrystallization annealing temperature on carbide precipitation, microstructure, and mechanical properties in Fe–18Mn–0.6 C–1.5 Al TWIP steel. Materials Science and Engineering: A, 2010. 527(3): p. 745-751.
[30]. Curtze, S. and V.-T. Kuokkala, Dependence of tensile deformation behavior of TWIP steels on stacking fault energy, temperature and strain rate. Acta materialia, 2010. 58(15): p. 5129-5141.
[31]. A. Dumay, J.-P. Chateau, S. Allain, S. Migot, O. Bouaziz, Influence of addition elements on the stacking-fault energy and mechanical properties of an austenitic Fe–Mn–C steel. Materials Science and Engineering: A, 2008. 483: p. 184-187.
[32]. Goodhew, P., Annealing twin formation by boundary dissociation. Metal Science, 1979. 13(3-4): p. 108-112.
[33]. R. Ueji, N. Tsuchida, D. Terada, N. Tsuji, Y. Tanaka, A. Takemura, K. Kunishige, Tensile properties and twinning behavior of high manganese austenitic steel with fine-grained structure. Scripta Materialia, 2008. 59(9): p. 963-966.
[34]. T. Roland, D. Retraint, K. Lu, J. Lu, Fatigue life improvement through surface nanostructuring of stainless steel by means of surface mechanical attrition treatment. Scripta Materialia, 2006. 54(11): p. 1949-1954.
[35]. Bouaziz, O., S. Allain, and C. Scott, Effect of grain and twin boundaries on the hardening mechanisms of twinning-

[DOI: 10.22068/ijmse.2937]

induced plasticity steels. Scripta Materialia, 2008. 58(6): p. 484-487.
[36]. Sajjad Amirkhanlou, Masoomeh Askarian, Mostafa Ketabchi, Navvid Azimi, Nader Parvin, Fernando Carreño, Gradual formation of nano/ultrafine structure under accumulative press bonding (APB) process. Materials Characterization, 2015. 109: p. 57-65.
[37]. Hamada, A., L. Karjalainen, and M. Somani, The influence of aluminum on hot deformation behavior and tensile properties of high-Mn TWIP steels. Materials Science and Engineering: A, 2007. 467(1-2): p. 114-124.
[38]. Jin, J.-E. and Y.-K. Lee, Effects of Al on microstructure and tensile properties of C-bearing high Mn TWIP steel. Acta Materialia, 2012. 60(4): p. 1680-1688.
[39]. Majid Abbasi, Shahram Kheirandish, Yosef Kharrazi, Jalal Hejazi, The fracture and plastic deformation of aluminum alloyed Hadfield steels. Materials Science and Engineering: A, 2009. 513: p. 72-76.
[40]. Motomichi Koyama, Yusuke Yamamura, Rinqing Che, Takahiro Sawaguchi, Kaneaki Tsuzaki, Hiroshi Noguchi, Comparative study on small fatigue crack propagation between Fe-30Mn-3Si-3Al and Fe-23Mn-0.5 C twinning-induced plasticity steels: Aspects of non-propagation of small fatigue cracks. International Journal of Fatigue, 2017. 94: p. 1-5.
[41]. Penghui Ma, Lihe Qian, Jiangying Meng, Shuai Liu, Fucheng Zhang, Influence of Al on the fatigue crack growth behavior of Fe–22Mn–(3Al)–0.6 C TWIP steels. Materials Science and Engineering: A, 2015. 645: p. 136-141.
[42]. Elber, W., The significance of fatigue crack closure, in Damage tolerance in aircraft structures. 1971, ASTM International.
[43]. T. Niendorf, F. Rubitschek, H.J. Maier, J. Niendorf, H.A. Richard, A. Frehn, Fatigue crack growth—Microstructure relationships in a high-manganese austenitic TWIP steel. Materials Science and Engineering: A, 2010. 527(9): p. 2412-2417.

[DOI: 10.22068/ijmse.2937]